



OPEN

In Vitro Hematological and *In Vivo* Vasoactivity Assessment of Dextran Functionalized Graphene

SUBJECT AREAS:

IMMUNOTOXICITY

CELL-PARTICLE INTERACTIONS

SYNTHESIS OF GRAPHENE

DRUG DELIVERY

Sayan Mullick Chowdhury¹, Shruti Kanakia¹, Jimmy D. Toussaint¹, Mary D. Frame¹, Anthony M. Dewar¹, Kenneth R. Shroyer², William Moore³ & Balaji Sitharaman¹Received
21 June 2013Accepted
12 August 2013Published
4 September 2013Correspondence and
requests for materials
should be addressed to
B.S. (balaji.sitharaman@
stonybrook.edu)¹Department of Biomedical Engineering, ²Department of Pathology, ³Department of Radiology Stony Brook University, Stony Brook, NY.

The intravenous, intramuscular or intraperitoneal administration of water solubilized graphene nanoparticles for biomedical applications will result in their interaction with the hematological components and vasculature. Herein, we have investigated the effects of dextran functionalized graphene nanoplatelets (GNP-Dex) on histamine release, platelet activation, immune activation, blood cell hemolysis *in vitro*, and vasoactivity *in vivo*. The results indicate that GNP-Dex formulations prevented histamine release from activated RBL-2H3 rat mast cells, and at concentrations ≥ 7 mg/ml, showed a 12–20% increase in levels of complement proteins. Cytokine (TNF-Alpha and IL-10) levels remained within normal range. GNP-Dex formulations did not cause platelet activation or blood cell hemolysis. Using the hamster cheek pouch *in vivo* model, the initial vasoactivity of GNP-Dex at concentrations (1–50 mg/ml) equivalent to the first pass of a bolus injection was a brief concentration-dependent dilation in arcade and terminal arterioles. However, they did not induce a pro-inflammatory endothelial dysfunction effect.

Graphene, a two-dimensional carbon nanostructure, due to its unique physiochemical properties, has shown potential for a variety of materials, electronic and biomedical applications^{1–3}. Specifically, graphene nanoparticles called graphene nanoplatelets, that can be synthesized in macroscopic amounts using the modified Hummer's method have shown promise as multifunctional nanoparticle for imaging^{4,5}, targeted drug delivery^{4,6–8}, gene delivery⁹, tissue engineering^{10,11}, and photodynamic/photothermal therapy^{12–14}. Development of graphene nanoparticles for any *in vivo* application requires thorough assessment of their toxicity and biocompatibility. In the case of graphene, relatively little work has been done to assess the toxic effects *in vitro*^{15–17} and *in vivo*^{18,19} compared to other carbon nanostructures^{20,21}. Most of the reports are on graphene nanoplatelets prepared by the modified Hummer's method or variations of this method. Recently, the *in vitro* cytotoxicity of graphene nanoribbons synthesized via the longitudinal unzipping of carbon nanotubes was reported³. These reports indicate that graphene nanoparticles, depending on their chemical composition and synthesis method, show diverse effects on cells and tissues. For any *in vivo* application, the systemic distribution of these nanoparticles in the circulatory system will lead to their interaction with hematological components and vasculature. Yet, no studies to date have systematically examined the effects of aqueous suspensions of graphene on the hematological system and vasculature.

Recently, we have synthesized and characterized highly water-soluble graphene nanoplatelets non-covalently functionalized with the natural polymer dextran (hereafter called GNP-Dex) for use as an MRI contrast agent²². In the present study, we evaluate *in vitro* and *in vivo* the hematological and vasoactive effects of GNP-Dex. *In vitro*, we investigate the histamine release from a rat basophilic cell line, platelet activation, complement activation, cytokine release and cell hemolysis in whole human blood after treatment with GNP-Dex. *In vivo*, using a hamster cheek pouch model, we examine the vasoactive response to GNP-Dex.

Results

Atomic force microscopy. Figure 1A shows a representative Atomic force microscopy (AFM) image of several GNP-Dex particles on silicon wafer. Figure 1B is a representative higher magnification image of an individual GNP-Dex nanoparticle with a diameter of 81.3 nm. Analysis of these and other AFM images indicated that the morphology of individual GNP-Dex nanoparticles were discoids with diameter between 60–100 nm and thickness of ~ 2 –4 nm.

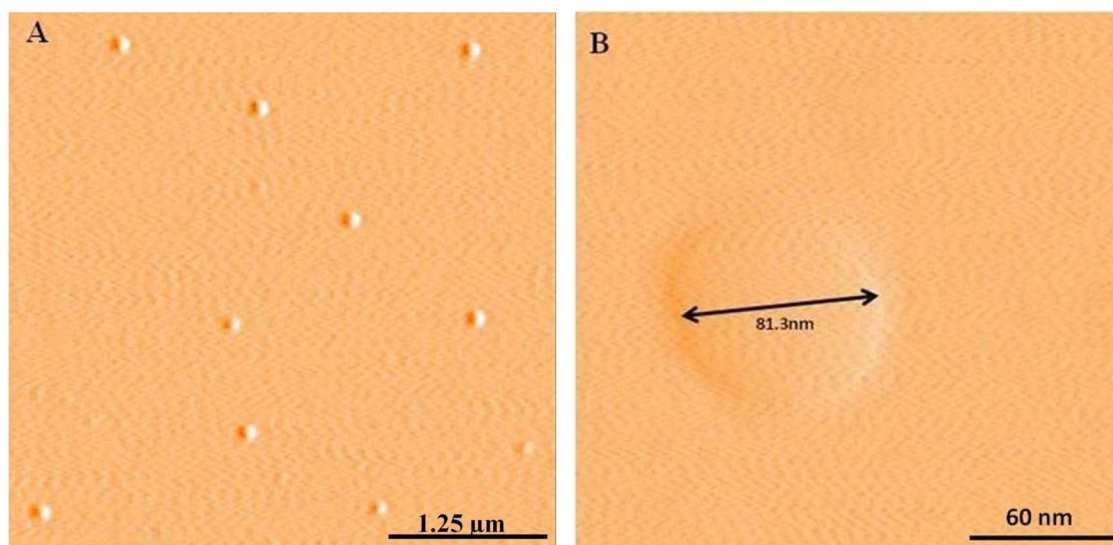


Figure 1 | Representative (A) Low resolution AFM image of GNP-Dex nanoparticles. (B) A magnified image of a GNP-Dex nanoparticle. Scale Bars (A) 1.25 μm , (B) 60 nm.

Histamine release assay. In this assay, histamine released from activated (with antibody) and induced (with an antigen) mast cells is extracted and quantified by conjugating it to O-Pthalaldehyde (OPT) to produce a fluorescent conjugate. Figure 2 shows the histamine release from activated (with anti 2,4-dinitrophenol(DNP) IgE) and induced (with 2,4 Dinitrophenyl-bovine serum albumin (DNP-BSA)) RBL-2H3 cells treated with the three concentrations of GNP-Dex, dextran (at 0.4 mg/ml and 4 mg/ml) or untreated. The results are expressed as a percentage of histamine released from activated but un-induced cells (i.e not treated with DNP-BSA). Induced cells treated with 3 mg/ml, 7 mg/ml and 10 mg/ml GNP-Dex showed $\sim 7\%$, $\sim 11\%$ and $\sim 15\%$ higher histamine release, respectively, compared to un-induced cells. Cells treated with only DNP-BSA showed $\sim 37\%$ increase in histamine release compared to un-induced cells. Induced cells treated with 0.4 mg/ml and 4 mg/ml dextran showed $\sim 16\%$ and $\sim 18\%$ higher histamine release, respectively, compared to uninduced controls.

Platelet activation assay. This assay is based on the principle that on activation (and ultimately aggregation) blood platelets release platelet factor 4 (PF₄), a 70 amino acid protein which has an anti heparin function in the circulatory system thus aiding blood clotting and platelet aggregation²³. The ELISA kit used detects presence of PF₄ in plasma using an anti PF4 antibody. Figure 3 shows the PF₄ released from the two different human blood samples treated to the three concentrations of GNP-Dex. The results are expressed as a percentage of PF₄ release in untreated blood. Treatment with the different GNP-Dex concentrations showed no statistically significant difference in PF₄ release in both blood sample 1 and 2.

Complement activation. The SC5b-9 or terminal complement complex assay is based on the principle that SC5b-9 protein is produced after activation of classical, lectin or alternate pathway of complement activation²⁴. The assay kit uses a monoclonal antibody targeted to the C9 ring of SC5b-9 to measure the concentration of the

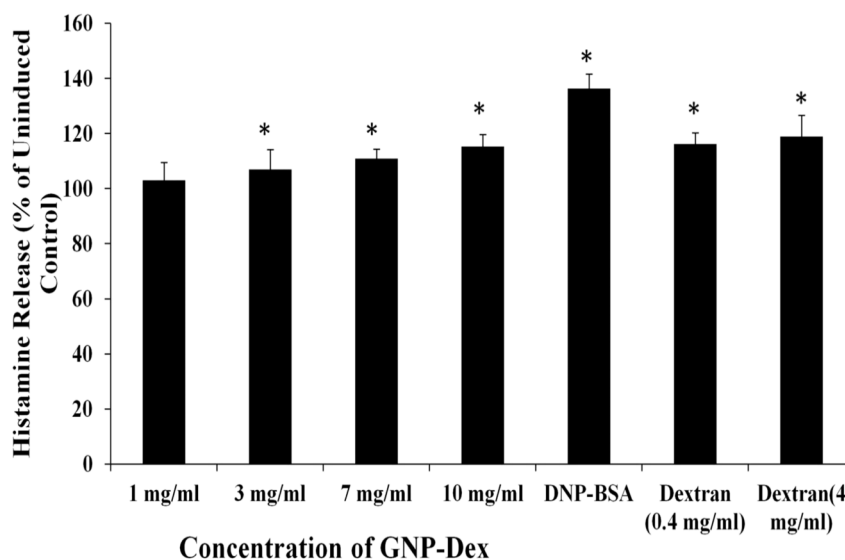


Figure 2 | Histamine release from activated and induced RBL-2H3 cells treated with GNP-Dex (1-10 mg/ml) or dextran only (0.4 mg/ml and 4 mg/ml) formulations for 45 min. Data are presented as mean \pm SD (n = 6 per group). * = $p < 0.05$ between treatment groups and uninduced control.

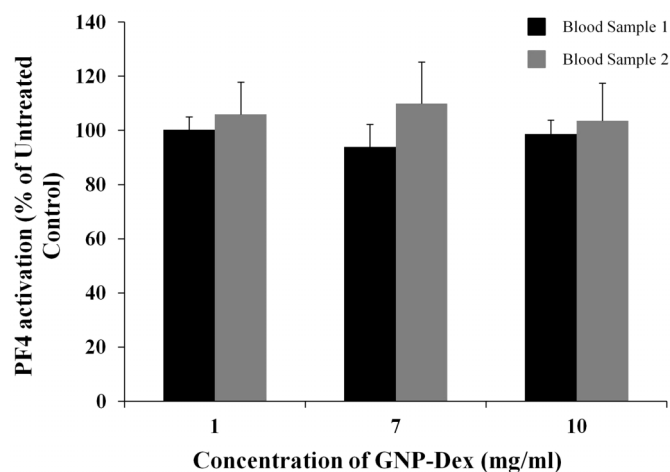


Figure 3 | Platelet activation assay presented in terms of PF₄ production in whole human blood from two individuals incubated at 1–10 mg/ml GNP-Dex concentrations for 45 min. Data are presented as mean \pm SD (n = 4 per group). * = $p < 0.05$ between untreated control and treatment group.

complex in plasma samples collected from blood treated with GNP-Dex formulations. Figure 4A shows the SC5b-9 produced in human blood samples from two different individuals when treated with 1 mg/ml, 7 mg/ml and 10 mg/ml GNP-Dex formulations. Results are expressed as percentage of control SC5b-9 levels in untreated blood. Blood sample 1 showed a $\sim 20\%$ increase in levels of SC5b-9 when treated with 10 mg/ml GNP-Dex. Lower concentrations (1 and 7 mg/ml) did not show statistically significant difference in SC5b-9. Blood sample 2 showed a $\sim 12\%$ increase in SC5b-9 levels, when treated with 7 mg/ml and 10 mg/ml GNP-Dex. 1 mg/ml GNP-Dex did not show statistically significant difference in SC5b-9 level.

The Bb assay which quantifies the activation of alternate pathway, is based on the principle that Bb (a fragment of Factor B cleaved by Factor D) is formed only when the alternate complement pathway is activated²⁵. This assay kit uses a monoclonal antibody against the Bb

protein to quantify the extent of alternate complement pathway activation. Figure 4B represents Bb release on treatment of blood samples from two different individuals to 0.4 mg/ml, 2.8 mg/ml and 4 mg/ml dextran. Results are expressed as percentage of control Bb levels in untreated blood. Blood sample 1 showed $\sim 11\%$ and $\sim 25\%$ increase in levels of Bb when treated with 2.8 mg/ml and 4 mg/ml solutions of dextran. Blood sample 2 showed $\sim 23\%$ and $\sim 37\%$ increase in levels of Bb protein when treated with 2.8 mg/ml and 4 mg/ml dextran. 1 mg/ml GNP-Dex did not show statistically significant difference in Bb protein in both blood samples.

Cytokine release. The Human TNF-Alpha (Tumor necrosis factor-Alpha) and IL-10 (Interleukin 10) release assays are based on the principle that, upon exposure to an irritant, or foreign particles and pathogens, cells of the innate immune system release pro-inflammatory and anti-inflammatory cytokines²⁶. A balance between these two kinds of cytokines is maintained depending on the type of irritant or pathogen encountered by the immune system²⁷. Thus, a change in the equilibrium of pro- and anti-inflammatory cytokine (i.e an increase or decrease of plasma concentration) suggests that the immune system has been activated. Figure 5A shows the TNF-Alpha produced in human blood samples from two different individuals when treated with 1 mg/ml, 7 mg/ml and 10 mg/ml GNP-Dex formulations. Results are expressed as percentage of control TNF-Alpha levels in untreated blood. Blood sample 1 showed $\sim 7\%$ increase in TNF-Alpha levels compared to untreated controls when exposed to 1 mg/ml GNP-Dex. However, higher concentrations did not show any statistically significant difference compared to the untreated control. Blood sample 2 did not show significant changes in TNF-Alpha levels when exposed to 1–10 mg/ml GNP-Dex. Figure 5B shows the IL-10 secreted in human blood samples from two different individuals after treatment with 1 mg/ml, 7 mg/ml and 10 mg/ml GNP-Dex formulations. Results are expressed as percentage of control IL-10 levels in untreated blood. Blood sample 1 did not show significant changes in IL-10 levels when exposed to upto 10 mg/ml GNP-Dex. Blood sample 2 showed a $\sim 11\%$ decrease in IL-10 levels compared to untreated controls when exposed to 1 mg/ml GNP-Dex. Higher concentrations did not show any statistically significant difference compared to the untreated control.

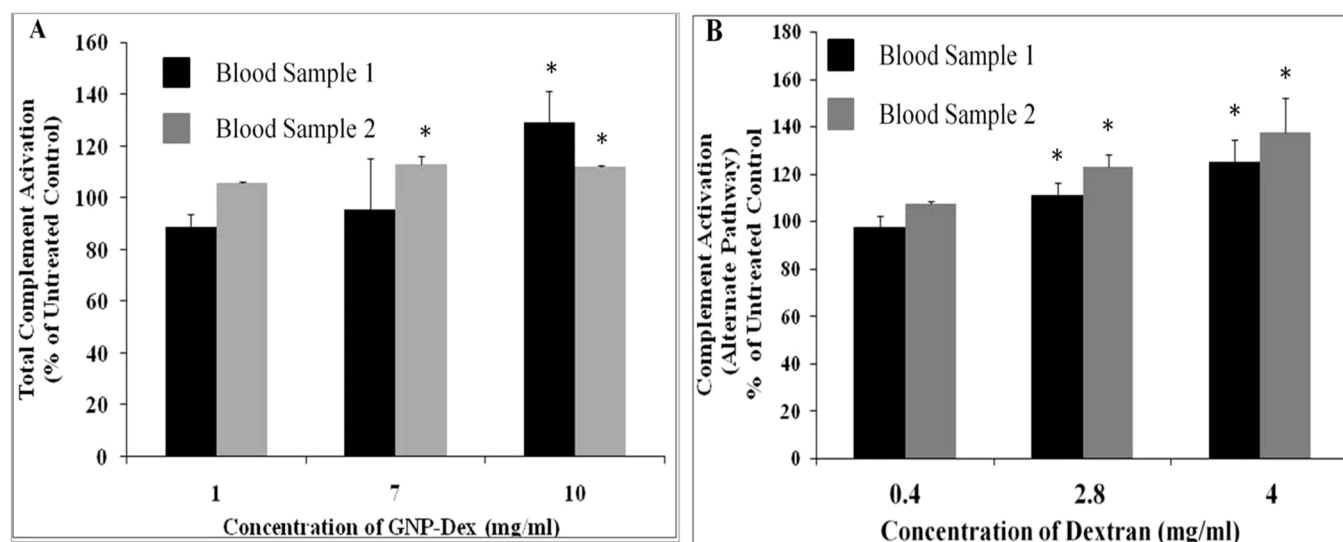


Figure 4 | (A) Total complement activation assay presented in terms of SC5b-9 protein production in human whole blood from two individuals treated with various GNP-Dex (1–10 mg/ml) concentrations. (B) Alternate complement pathway activation in terms of Bb protein production in two human whole blood samples treated with various concentrations of dextran only (0.4–4 mg/ml). Data are presented as mean \pm SD (n = 4 per group). * = $p < 0.05$ between untreated control and particular treatment group.

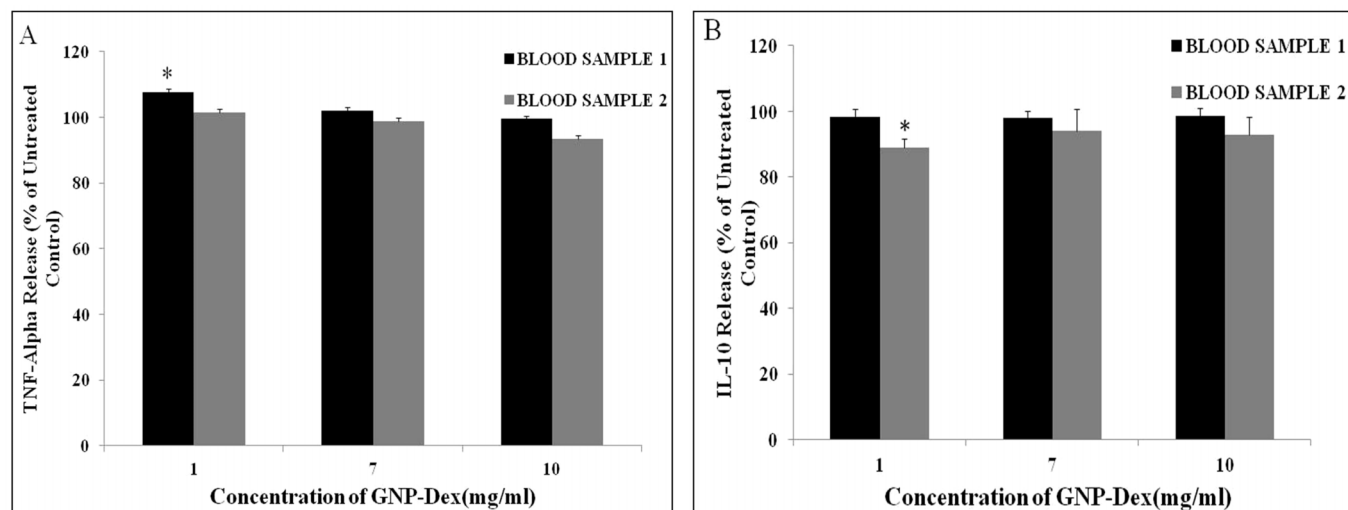


Figure 5 | (A) Pro-inflammatory cytokine release assay presented in terms of TNF-Alpha release in whole human whole blood from two individuals treated with various GNP-Dex (1–10 mg/ml) concentrations. (B) Anti-inflammatory cytokine release assay presented in terms of IL-10 release in whole human blood from two individuals treated with various GNP-Dex (1–10 mg/ml) concentrations. Data are presented as mean \pm SD (n = 4 per group). * = $p < 0.05$ between untreated control and particular treatment group.

Blood cell hemolysis. Cell morphology analysis. Figures 6A–C are representative bright-field images of red (red arrows) and white blood cells (black arrows) treated with 1 mg/ml, 7 mg/ml and 10 mg/ml GNP-Dex solutions. Figure 6D is a representative image of untreated control cells. Figure 6E is a representative image of blood cells treated with polyethyleneimine. Treated cells showed no difference in cell morphology compared to untreated (control) blood cells. No particles were identified adhering to the surface of the blood cells also. In comparison, polyethyleneimine (PEI) treated cells showed changes in morphology and visible aggregation.

Hemoglobin release analysis. This colorimetric method relies on the principle that hemolysis of red blood cells lead to the release of hemoglobin which can be converted to cyanomethemoglobin using ferricyanide in presence of bicarbonate. Cyanomethemoglobin can be quantified by measuring its absorbance at 540 nm²⁸. Figure 6F shows the supernatant obtained after exposure of blood to GNP-Dex concentrations for 45 minutes followed by centrifugation of the mixture at 2500 rpm for 10 minutes. Figure 6G shows the colorimetric quantification of cyanomethemoglobin in the supernatants. Absorbance values of the supernatant were 0.06, 0.10 and 0.11 from 1 mg/ml, 7 mg/ml and 10 mg/ml GNP-Dex treated red blood cells, 0.06 for untreated cells and 0.68 for Triton X-100 treated cells.

Vasoactivity. Figure 7A shows a representative image from hamster cheek pouch tissue and illustrates the micropipette exposure technique. Figure 7B shows vasodilation of two classes of small arterioles: arcade and terminal arterioles with exposure to GNP-Dex formulations. Baseline diameters were measured to be $23 \pm 9 \mu\text{m}$ (mean \pm SD) in arcade arterioles and $8 \pm 1.4 \mu\text{m}$ in terminal arterioles. Exposure of the arterioles to the two lowest concentrations (i.e 0.1 and 0.5 mg/ml) did not significantly alter arteriolar diameter. Of note, exposure to 10 or 50 mg/ml was not statistically different from each other. The control, dextran, at low dose (3.5 mg/ml) caused a dilation of $4 \pm 5\%$ (mean \pm SD) in arcade arterioles and $19 \pm 17\%$ in terminal arterioles. Higher dose dextran alone (35 mg/ml) caused dilation of $23 \pm 14\%$ in arcade arterioles and $63 \pm 29\%$ in terminal arterioles. Thus, a large component of the vasoactive effect could be attributed to the dextran coating itself.

Of greater importance is the absence of a residual effect to the vasculature following brief exposure to the GNP-Dex formulations.

Specifically, we tested endothelial dependent dilation (acetylcholine) and endothelial independent dilation (adenosine) or constriction (phenylephrine) before and after exposure to 50 mg/ml GNP-Dex. Exposure of 50 mg/ml GNP-Dex to these arterioles did not significantly alter any dilatory or constrictor responses, suggesting that there was no residual inflammatory or compromising effect.

Discussion

The objective of this study was to investigate the effects of GNP-Dex formulations on various hematological and vascular constituents. *In vitro* and *in vivo* toxicity and biocompatibility of nanoparticles is necessary for their development for any *in vivo* application²⁹. For future therapeutic and diagnostic applications, the GNP-Dex particles, administered by intravenous, intramuscular or intraperitoneal injections will, interact with the the circulatory system. During this interaction, the formulation will come in contact with blood cells, clotting factors, allergen response system, immune system and blood vessels. Thus, we have investigated the effects of GNP-Dex formulations on histamine release (indicator of-allergic response), platelet activation (which can lead to unnatural clotting), complement activation (which can lead to an immune response), blood cell hemolysis *in vitro*, and vasoactivity *in vivo*.

For the *in vitro* studies, the rationale for using GNP-Dex concentrations of 1 mg/ml, 7 mg/ml and 10 mg/ml is as follows. The lethal dose (LD₅₀) values for a single bolus injection of GNP-Dex still need to be determined. We have estimated that future *in vivo* preclinical safety (acute toxicity) studies to establish the therapeutic dosages would require their administration at a range of dosages; from 50 mg/kg upto possibly ≥ 500 mg/kg body weight of the small animal²². If the GNP-Dex are injected at a dose of 50 or 500 mg/kg body weight of a 250 g rat (total circulating blood volume 12–13 ml), its steady state blood concentration after the first pass would be ~ 1 or 10 mg/ml, respectively. Thus, the three concentrations bracket the low to high steady state blood concentrations. For *in vivo* vasoactivity studies, an additional GNP-Dex concentration of 50 mg/ml was included since, for applications requiring its intravenous administration, based on indicator dilution profiles and relative cardiac output³⁰, we know that the first pass of GNP-Dex is likely to be 30–50 mg/ml before it achieves the above steady state blood concentration. Immediately after its first injection (1st pass of the agent), it will be present at significantly higher concentrations, and then within

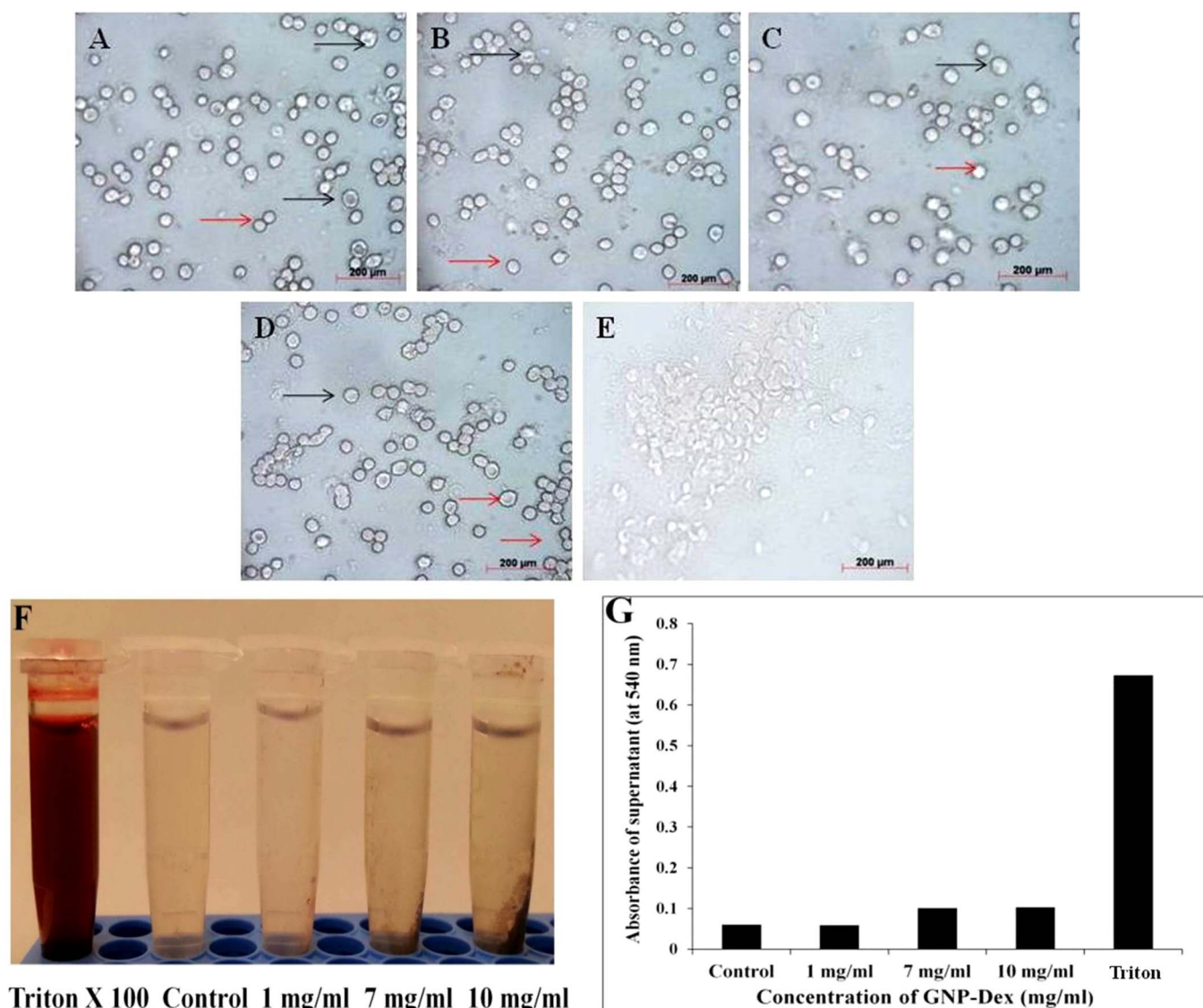


Figure 6 | (A–C) Representative images of blood cells (RBC shown with red arrows and WBC shown with black arrows) treated with 1 mg/ml, 7 mg/ml and 10 mg/ml GNP-Dex, respectively. (D) Representative image of untreated control blood cells. (E) Representative image showing hemolysed cells treated with poly ethylene imine; a known hemolytic agent. (F) Supernatants obtained after centrifuging red blood cell suspensions treated with GNP-Dex formulations, or Triton \times 100 for 45 minutes. (G) Absorbance values of the supernatants at 540 nm obtained after conversion of the hemoglobin present to cyanomethemoglobin. Scale bar = 200 μ m for images (A–E).

minutes uniformly distribute within the blood volume to reach a lower steady state concentration.

The average size of the GNP-Dex determined by the analysis of the low and high resolution AFM images was \sim 100 nm. Further, the thickness of the GNP-Dex complex was \sim 2–4 nm. The AFM images are similar to this previous report that describes the complete synthesis and physicochemical characterization of the GNP-Dex formulation²². That report also showed that the dextran uniformly coats the GNPs, GNP-Dex contains dextran at 40% by weight, are hydrophilic, soluble in water at concentrations upto 100 mg/ml, stable in deionized water and biological buffers, possess viscosity values within the range of blood viscosity (between 3–4 cP at 37°C), and does not show non-specific blood protein absorption.

Histamine release from basophil and mast cells is a basic immune response triggered by an allergen, and thus is an excellent marker for evaluating the propensity of a material to induce an allergic reaction. Treatment of rat peritoneal mast cells with high molecular weight dextrans (>10 KDa) have been shown to invoke histamine release³¹. Since 10 KDa dextran was used for synthesis of GNP-Dex, we

examined the allergenic potential of GNP-Dex by treating activated and induced RBL-2H3 basophilic cells with it (Figure 2). In the absence of GNP-Dex treatment, the induced cells showed \sim 36% increase in histamine release compared to untreated, uninduced control cells. However, treatment of the cells with 10 mg/ml GNP-Dex (which contains \sim 4 mg/ml dextran) decreased the histamine release to \sim 15%, which was equivalent to the histamine release upon treatment with 0.4 mg/ml (\sim 16%) and 4 mg/ml (\sim 18%) dextran. Lower concentration GNP-Dex treatment resulted in further decrease of histamine release from the induced cells. One mg/ml GNP-Dex (which contains \sim 0.4 mg/ml dextran) did not show statistically significant difference in histamine release from the uninduced control cells. Thus, it can be inferred that the decrease in histamine release is not due to the dextran alone, and low concentrations of GNP-Dex possibly have an anti-allergic effect. IgE-induced histamine release occurs mainly as membrane bound vesicles through exocytosis from the plasma membrane³². The GNP-Dex nanoparticles may be preventing this exocytosis, more at lower concentrations than at higher concentrations. Additional studies are needed to test this hypothesis.

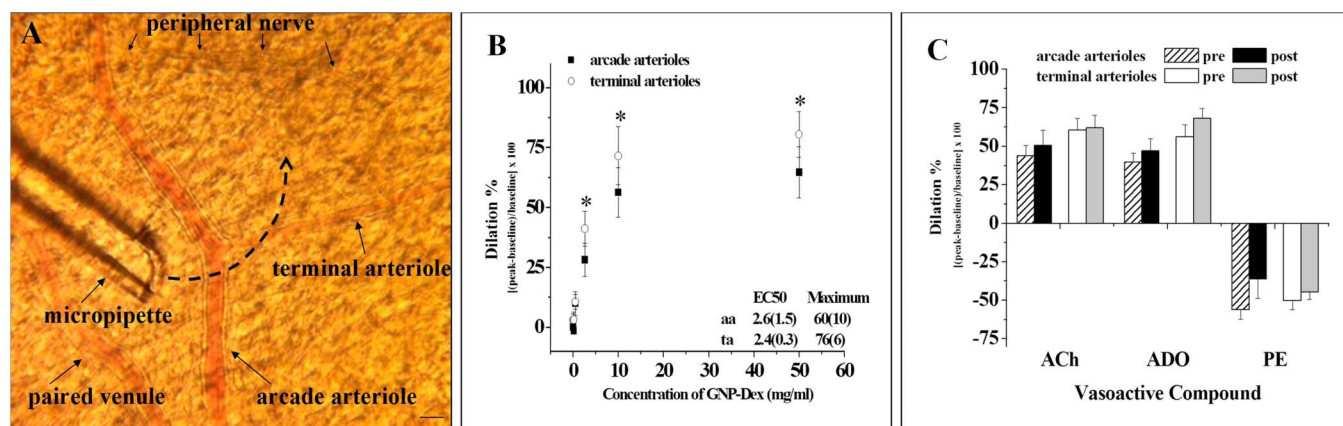


Figure 7 | (A) Micrograph from hamster cheek pouch (shown with normal resting tone), depicting the terminal arteriole, and arcade arteriole. The micropipette was placed so that the contents passed over the arterioles of interest and then washed away in the flowing tissue bath as depicted by the dashed arrows. Scale bar = 20 μ m. (B) Dose dependent dilation (mean \pm sem) to GNP-Dex for arcade and terminal arterioles. The fitted EC50 and maximal dilation are shown in the figure as mean (sem). $n = 8$. * indicates both arcade and terminal arterioles exhibit a significant dilation, $p < 0.05$. (C) Diameter change (mean \pm sem) before (pre) and 15 minutes after (post) exposure to 50 mg/ml GNP-Dex for arcade and terminal arterioles in response to 10^{-4} mol/L ACh (acetylcholine), ADO (adenosine) or PE (phenylephrine). $n = 8$.

Platelet activation in the circulatory system can lead to formation of clots in the blood vessels which may result in myocardial infarction or stroke³³. A recent study has also shown that graphene oxide nanosheets induce thrombus¹⁵. Hence, we tested the blood of two individuals for platelet activation in response to 1 mg/ml, 7 mg/ml and 10 mg/ml suspensions of GNP-Dex (Figure 3). No significant changes were observed in the levels of PF₄ in whole blood even at the highest concentration of GNP-Dex indicating that GNP-Dex did not induce platelet activation and aggregation. These results are significantly different than those of other carbon nanostructures such as single walled carbon nanotubes (SWCNTs) and multi-walled carbon nanotubes (MWCNTs) which have been shown to activate blood platelets leading to unwanted platelet aggregation³⁴. However, those studies were performed on pristine single- and multi-walled carbon nanotubes.

Activation of small proteins of the complement system is an immune response that regulates the functioning of other immunity mechanisms²⁴. The activation mechanism is generally triggered by foreign proteins and polysaccharides originating from microbes, and result in cytokine release²⁴. The activation of complement system can take place through the classical pathway, alternative pathway or lectin pathway²⁴. Unwanted activation of the complement system on exposure to nanoparticles could result in hypersensitivity reactions as previously observed with pegylated Doxil[®] liposomal nanoparticles³⁵. A previous study has shown that unfunctionalized graphene oxide can activate the complement system³⁶. Hence we tested the level of complement activation on exposure to GNP-Dex solutions. The results from total complement activation assay on blood sample 1 show that treatment of GNP-Dex at concentrations up to 7 mg/ml does not result in significant increase in Sc5b-9 levels. Exposure of 10 mg/ml GNP-Dex resulted in $\sim 20\%$ increases in the level of complement activation. Calculation of SC5b-9 concentration from the absorbance values and standard curve provided with the kit showed that the control Sc5b-9 concentration in untreated blood was ~ 395 ng/ml. A $\sim 20\%$ increase in this value is equal to Sc5b-9 protein concentration of ~ 474 ng/ml which falls within the normal limits of Sc5b-9 protein in humans (176–624 ng/ml)³⁷. Similarly, the results from total complement activation assay on blood sample 2 showed that treatment of 1 mg/ml GNP-Dex did not result in significant differences in complement activation compared to controls. However, exposure of 7 mg/ml and 10 mg/ml GNP-Dex resulted in $\sim 12\%$ increase in the level of complement activation at both concentrations. Calculation of SC5b-9 concentration showed that the

control Sc5b-9 concentration in untreated control blood was ~ 450 ng/ml. A $\sim 12\%$ increase in this value is equal to Sc5b-9 protein concentration of ~ 504 ng/ml which also falls within the normal limits of Sc5b-9 protein in humans³⁷. (Figure 4A) The results indicate that although higher concentrations of GNP-Dex (7 mg/ml and 10 mg/ml) resulted in small increase in complement activation, the degree of not complement activation was within normal limits for healthy individuals.

Prior studies have reported that nanoparticles coated with dextran (average molecular weight 10 KDa) can induce activation of the complement system through the alternate pathway³⁸. Since dextran accounts for $\sim 40\%$ by weight of GNP-Dex²², additional experiments were performed to investigate whether the $\sim 20\%$ and $\sim 12\%$ increase in total complement activation observed in the two blood samples were mainly due to the presence of dextran. In these experiments, the level of alternate complement pathway activation in blood was measured after treating the two blood samples with 0.4 mg/ml, 2.8 mg/ml and 4 mg/ml dextran (40% of 1 mg/ml, 7 mg/ml and 10 mg/ml GNP-Dex). At the two higher concentrations, blood sample 1 showed $\sim 11\%$ and $\sim 25\%$ increase, and blood sample 2 showed $\sim 23\%$ and $\sim 37\%$ increase in alternate pathway activation. Thus, it can be inferred that the dextran present in the GNP-Dex formulations contributed to the observed increase in complement activation (Figure 4B).

A common response of the immune system on coming in contact with an irritant or pathogen is to induce inflammation³⁹. The main mediators for inflammation are macrophages and other cells of the innate immune system which release pro-inflammatory or anti-inflammatory cytokines⁴⁰. In a normal healthy individuals, a balance between pro-inflammatory and anti-inflammatory cytokines is maintained²⁷. On introduction of an irritant, the pro-inflammatory cytokines get secreted in larger quantities compared to normal levels. The opposite applies for immune suppression; anti-inflammatory cytokines are produced in larger quantities. Thus, an increase in production of either type of cytokine indicates a deviation from homeostasis. In a recent study, graphene oxide nanosheets have been shown to induce the release of pro-inflammatory cytokines⁴¹. Thus, we tested the release of pro-inflammatory cytokine TNF-Alpha and anti-inflammatory cytokine IL-10 after exposure to 1–10 mg/ml GNP-Dex (Figure 5A and 5B). Results show that, compared to untreated control cells, after 1 mg/ml exposure of GNP-Dex, blood sample 1 showed $\sim 7\%$ increase in TNF-Alpha levels (~ 7 pg/ml), and blood sample 2 showed a $\sim 11\%$ decrease in IL-10 levels (~ 1 pg/



ml). However, the resulting concentrations for both the increase and the decrease were within the normal healthy levels for humans (<15 pg/ml for TNF-Alpha and < 3 pg/ml for IL-10 as calculated from the standard curve)^{42,43}. There were no significant changes in the concentrations of both these cytokines after exposure to higher GNP-Dex concentrations.

The hemolytic potential of the nanoparticles when incubated with whole blood is an important part of investigating their hematological effects⁴⁴. Two common mechanisms leading to blood cell hemolysis are through reactive oxygen species (ROS) generation in presence of the cells and penetration of the cell membrane⁴⁴. We used two different methods to assess the hemolytic potential of GNP-Dex; cell morphology, and hemoglobin release analysis. The cell morphology analysis (Figures 6A–E) indicated that incubation of whole human blood with 1–10 mg/ml GNP-Dex did not result in hemolysis or change in morphology of red blood cells (red arrows in Figures 6A–D) or white blood cells (black arrows in Figures 6A–D) when compared to control (treated with phosphate buffered saline). The cell morphology analysis showed hemolysis of cells by PEI, a known hemolytic agent (Figure 6E). The hemoglobin release analysis (Figure 6F–G) corroborated the cell morphology analysis results. The red blood cells treated with 1–10 mg/ml GNP-Dex for 45 minutes showed minimal increase in hemoglobin release (absorbance increased from 0.059 in unexposed control to 0.103 in 10 mg/ml exposed GNP-Dex samples). In contrast, Triton × 100, a known hemolytic agent caused ~ 7 fold higher hemoglobin release compared to 10 mg/ml GNP-Dex (absorbance reading 0.675). These results are in contrast to recent reports on the hemolytic effects of MWCNTs and graphene nanoparticles^{45,46}. A study by Meng *et al.* on the hemolytic effects of functionalized MWCNTs indicated that, the hydrophobicity of the carboxylated and aminated MWCNTs leads to its adhesion to the hydrophobic cell membrane causing damage and lysis of the cells⁴⁵. Liao *et al.* showed that as-prepared graphene oxide nanoparticles (prepared by Hummer's method) or graphene sheets (prepared by hydrazine-free hydrothermal route) show variable hemolytic activity on red blood cells. The authors report that size and charge of graphene sheets (which depends on its method of synthesis) plays an important role on the amount of red blood cell hemolysis⁴⁶. The hemolysis effect was mitigated by coating the graphene nanoparticles with the biocompatible natural polymer chitosan; a linear polysaccharide⁴⁶. In the current study, the absence of hemolysis maybe due to biocompatible natural polymer dextran (a complex branched polysaccharide) coating which prevented the adhesion of GNP-Dex to red or white blood cell membrane (Figure 6A–D).

Although the *in vitro* results taken together indicate that the GNP-Dex show no adverse effects on the hematological components, additional *in vivo* hematological studies are necessary to obtain a complete assessment. Thus, intensive single and repeat dose hematological studies with the GNP-Dex in rodents are currently underway.

The effect of nanoparticles on vasoactivity is another important cardiovascular assessment. Here we have used the hamster cheek pouch model with extraluminal application of the formulations as an assay. At this level of the circulation, extraluminal application will expose both the vascular smooth muscle cells (discontinuously wrapped around the outside) and the abluminal surface of the endothelial cells. A large range of concentrations was tested (including very high doses) so that we could be certain that the first pass of the *i.v.* injected bolus would not cause long-lasting proinflammatory endothelial dysfunction. Based on indicator dilution methodology³⁰, we know that the first pass of the agent is likely to be not more than 30–50 mg/ml, thus our highest dosage tested was 50 mg/ml. The time duration of this first pass is dependent on the cardiac output. Typically, the first pass will take ~ 10–20 seconds, and uniform dispersion in the blood would occur in ~ 2 minutes³⁰. Additionally,

most vasoactive responses occur within 10–15 seconds of exposure to the agent. Thus, the exposure time of the GNP-Dex was extended to 30 seconds. Finally, testing the range of concentrations is critical since it is well known that long-lasting pro-inflammatory responses can be induced if inflammatory agents are exposed to the vasculature even briefly (seconds)^{47–52}. The exposure to GNP-Dex to the terminal or arcade arterioles caused a dose dependent dilation and yielded statistically similar EC₅₀ (half of maximal dilation observed, noted on Figure 7B) and maximal dilation values in both. The EC₅₀ was calculated ~ 2.5 mg/ml and this concentration induced 30–40% dilation in these arterioles - significantly different from baseline. Maximal dilation was observed at 10 mg/ml GNP-Dex concentration in either class of arterioles, which may be attributed to the dextran coating alone. Importantly, the dilations after GNP-Dex exposure were transient, and recovery was immediately.

Next, we tested whether exposure to the dextran or dextran functionalized GNP-Dex induced a long lasting change in vasoactive capability. After exposure to the highest GNP-Dex concentration (50 mg/ml), there was no evidence of endothelial dysfunction (normal dilation to acetylcholine). Further, the normal vasoactive capability to dilation or constriction was retained. Thus, we infer that endothelial dysfunction did not occur following GNP-Dex exposure. To the best of our knowledge, there have been no studies that have investigated the vasoactivity of graphene nanoparticle solutions. The results with GNP-Dex are significantly different from our recent study that investigated the vasoactivity of SWCNTs coated with the biocompatible amphiphilic polymer N-(carbonyl-methoxy-polyethylene glycol 2000)-1, 2-distearoyl-sn-glycero-3-phosphoethanolamine (PEG-DSPE) on terminal and arcade arterioles in hamsters and rats. Contrary to our findings with GNP-Dex, short term exposure of PEG-DSPE coated SWCNT formulations (aggregated or non-aggregated forms) can cause endothelial dysfunction in the arterioles under bolus dosing conditions, and at significantly lower dosages (50 µg/ml) compared to GNP-Dex (50 mg/ml)⁵³.

Methods

Synthesis of GNP-Dex. Oxidized graphene nanoplatelets (GNPs) were prepared according to a previously described method⁵. Briefly, graphite flakes were pre-oxidized using formic acid and washed with acetone. These pre-oxidized graphite particles were oxidized with sulphuric acid and potassium permanganate to obtain graphite oxide. The graphite oxide particles obtained were purified by dialysis and exfoliated in water by bath sonication (Ultrasonicator FS30H, Fischer Scientific, Pittsburgh, PA) to obtain GNPs. The GNPs were non-covalently functionalized with dextran (Pharmacosmos, MW 10000 Da) to synthesize GNP-Dex using a method previously described by Kanakia *et al.*²². GNPs and dextran were mixed in water at a 1 : 10 weight ratio, and bath sonicated for 30 minutes followed by addition of ammonium hydroxide (NH₄OH). This mixture was stirred at 95 °C for 3 hours. The particles were centrifuged at 1000 rpm for 15 minutes, and the supernatant was transferred to fresh tubes to obtain water soluble GNP-Dex. The supernatant was lyophilized, and the solid powder was resuspended in deionized water at desired concentrations.

Atomic force microscopy. GNP-Dex samples diluted to 10 µg/ml using a 1 : 1 ethanol water mixture were probe sonicated, (Cole Parmer Ultrasonicator LPX 750) and centrifuged at 1000 rpm for 15 minutes. The supernatant was collected and drop cast onto silicon wafers and dried overnight before imaging. AFM images were obtained using a Nano Surf Easy Scan 2 AFM (NanoScience Instruments Inc, Phoenix, AZ), operating in tapping mode, using a V-shaped cantilever.

Cell culture. RBL-2H3 rat basophilic cells were used in the histamine release experiments. The cell line were obtained from ATCC (Manassas, VA, USA) and grown in MEM medium with Sodium pyruvate, non-essential amino acids and supplemented with 15% fetal bovine serum. 1% penicillin-streptomycin was used as antibiotic. Cells were incubated at 37 °C in a humidified atmosphere of 5% CO₂, and 95% air.

Histamine release. The histamine release assay was carried out using a previously reported method that involves a reaction between histamine and O-Pthalaldehyde (OPT) to quantify histamine release in activated rat mast cells⁵⁴. This assay was performed in three steps. In the first step, histamine released from activated RBL-2H3 cells with or without GNP-Dex treatment was extracted from alkalized HClO₄ treated cell media to an organic phase. In the second step, the extracted histamine was returned to aqueous phase. Finally, in the third step, the histamine was conjugated to



OPT to form a fluorescent product. The concentration of this fluorescent product was quantified with a spectrofluorometer using an excitation wavelength of 360 nm and emission wavelength of 450 nm. Briefly, RBL-2H3 cells were seeded into 48 well plates at the density of 10^4 cells per well. The experiment was performed 48 hours after cell seeding. The cells were washed twice with piperazine-N,N'-bis(2-ethanesulfonic acid) (PIPES) buffer, and incubated at 37°C for 1 hour with mouse monoclonal anti-2,4 dinitrophenyl (anti-DNP) IgE antibody (0.5 mg/ml) for sensitization. Following sensitization, wells were washed twice with PIPES buffer to remove excess antibody, and incubated with or without 1 mg/ml, 7 mg/ml and 10 mg/ml GNP-Dex and dextran (0.4 mg/ml and 4 mg/ml) for 15 min. The wells were then incubated with phosphatidylserine (10 µg/ml) for 5 minutes followed by DNP-BSA (0.1 µg/ml in 0.5 ml cell culture media) for 30 minutes to induce histamine release. The media (0.5 ml) was transferred to another tube containing 0.5 ml of 0.8 N HClO₄. To this mixture, 125 ml of 5 N NaOH (for alkalization), 0.4 g of NaCl and 2.5 ml of n-butanol was added and centrifuged at 1000 rpm for 3 min (for extraction of histamine into butanol). The upper organic phase was transferred to tubes containing 2 ml of 0.1 N NaOH saturated with NaCl, and centrifuged to remove contaminated materials from the organic phase. This process was repeated several times. The upper organic phase was transferred to tubes containing 1.8 ml 0.1 N HCl and 7.6 ml n-heptane (to return histamine into aqueous phase). 0.1 ml of 10 N NaOH was added to 1 ml of the lower aqueous phase. The histamine-OPT reaction was carried out by incubation with 0.1 ml of OPT (in 10 mg/ml methanol) for 4 min at room temperature, and the reaction was stopped by addition of 0.6 ml of 3 N HCl. The fluorescence of the histamine-OPT conjugate was assessed at 450 nm emission after excitation at 360 nm in a Cytofluor fluorescence multiwell plate reader (Series H4000 PerSeptive Biosystems, Framingham, MA). The fluorescence readings obtained from cells treated with GNP-Dex were compared to control readings from uninduced cells and cells treated with 0.4 mg/ml and 4 mg/ml dextran.

Platelet activation assay. The platelet activation assay in whole human blood treated with different concentrations (1–10 mg/ml) of GNP-Dex was carried out using an Immunoclone PF₄ ELISA kit (American Diagnostic Inc, Stamford, CT). Whole human blood (of 2 healthy male individuals, obtained from BioChemed, Winchester, VA) hereafter called blood sample 1 and blood sample 2 respectively, was treated with 1 mg/ml, 7 mg/ml and 10 mg/ml of the GNP-Dex formulation for 45 min. The GNP-Dex treated blood samples and untreated control samples were centrifuged at 2500 rpm for 30 minutes. The plasma collected from treatment and control samples was diluted 1:5 using a PF₄ sample diluent that contains a rheumatoid factor inhibitor. 200 µl of the diluted treated and control samples were added to appropriate wells in an antihuman PF₄ coated micro well strips provided with the kit and incubated for 1 hour. After incubation, the wells were washed five times with 300 µl of wash solution to remove non-specific proteins. 200 µl of anti PF₄-Horse radish peroxidase(HRP) immunoconjugate was then added to each well and incubated for 1 hour at room temperature. After incubation, the wells were washed five times with 300 µl of wash solution to remove excess immunoconjugate followed by addition of 200 µl of TMB substrate/peroxidase substrate (3, 3', 5, 5'-Tetramethylbenzidine), and incubated for 5 minutes at room temperature. Next, to each well, 50 µl of 0.45 M H₂SO₄ was added, and incubated for 10 minutes to terminate the reaction, as well as allow the color change to stabilize. Colorimetry readings were taken using a microwell plate reader (ELx 800, BIOTEK, Winooski, VT). Absorbance was measured at 450 nm.

Complement activation. The complement activation assay in whole human blood treated with different concentrations (1–10 mg/ml) of GNP-Dex was carried out using Microvue SC5b-9 and Bb plus ELISA kits (Quidel Corporation, San Diego, CA). Whole human blood (of 2 healthy male individuals, obtained from BioChemed, Winchester, VA) was treated with 1 mg/ml, 7 mg/ml and 10 mg/ml of the GNP-Dex formulation and 0.4 mg/ml, 2.8 mg/ml and 4 mg/ml dextran solutions respectively for 45 min. The treated and untreated blood samples were centrifuged at 2500 rpm for 30 minutes to isolate the plasma. The plasma collected was diluted five-fold (1:5) for blood sample 1 and three fold (1:3) for blood sample 2 using a specimen diluent. 100 µl of the diluted treated and untreated samples were added to wells in a SC5b 9/Bb coated micro well strip provided with the kit and incubated for 1 hour. Post incubation, all wells were washed five times with 300 µl of wash solution to remove unreacted proteins. 50 µl of anti SC5b9-HRP Immunoconjugate/Bb-HRP immunoconjugate was then added to each well, and incubated for 30 min at room temperature. After incubation, the wells were again washed five times with 300 µl of wash solution to remove excess immunoconjugate, followed by addition of 100 µl of TMB substrate/peroxidase substrate, and incubation for 15 minutes at room temperature. 100 µl of 0.45 M H₂SO₄ was added to each well to stop the reaction, incubated for 10 minutes to allow the color change to stabilize. The optical absorbance readings at 450 nm were taken using a microwell plate reader (ELx 800, BIOTEK, Winooski, VT). A standard curve obtained from standards provided with the kit was used to calculate plasma SC5b-9 values from the absorbance values obtained.

Cytokine release. Pro-inflammatory and anti-inflammatory cytokine release assay in whole human blood treated with different concentrations (1–10 mg/ml) of GNP-Dex was carried out using Human TNF-Alpha and IL-10 ELISA kits (Invitrogen, Grand Island, NY). Whole human blood (of 2 healthy male individuals, obtained from BioChemed, Winchester, VA) was treated with 1 mg/ml, 7 mg/ml and 10 mg/ml of the GNP-Dex formulation for 45 min. Untreated blood samples were used as control.

Treated and untreated blood samples were centrifuged at 2500 rpm for 30 minutes to isolate the plasma. 50 µl of the treated and untreated samples were added to wells in anti-TNF-Alpha/Anti IL-10 coated micro well strips provided with the kit along with 50 µl of incubation buffer and incubated for 2 hours. Post incubation, all wells were washed four times with 400 µl of wash solution to remove unreacted proteins. 100 µl of biotinylated anti-TNF Alpha/anti-IL 10 solution was added to the wells and incubated for 1 hour and 2 hours respectively following which the wells were washed 4 times with wash solution. 100 µl of Streptavidin-HRP conjugate was added to the wells and incubated for 30 minutes following which the wells were again washed 4 times with wash solution. 100 µl of stabilized chromogen solution provided with the kit was added to the wells and incubated for 30 minutes in the dark. 100 µl of stop solution was added to the wells to stop the reaction. Absorbance reading of each well at 450 nm was taken after subtracting values from the chromogen blank wells (100 µl stabilized chromogen solution and 100 µl stop solution) using an Infinite M200 multiwell plate reader (Tecan Group, Morrisville, NC). A standard curve obtained from standards provided with the kit was used to calculate plasma TNF Alpha/IL-10 values from the absorbance values obtained.

Blood cell hemolysis. Cell morphology analysis. One ml of whole human blood (BioChemed, Winchester, VA) was treated with 1 mg/ml, 7 mg/ml and 10 mg/ml of the GNP-Dex formulation for 45 min. GNP-Dex treated and untreated (Control) blood samples were centrifuged at 2500 rpm for 10 minutes, and the blood cell component (RBC, WBC) was separated from plasma. The blood cell components were diluted in 3 ml of isotonic buffer, and 10 µl of this solution was streaked onto a microscopic slide and fixed. The fixed slides were viewed under a high power bright-field microscope at 630 × (AxioLab Microscope, Carl Zeiss, Thornwood, NY). The morphology of RBC's and WBC's treated with GNP-Dex was compared to RBCs and WBCs treated with polyethyleneimine (PEI), a known hemolytic agent (positive control), and RBC's and WBC's from saline treated normal blood (negative control).

Hemoglobin release analysis. Hemoglobin released due to hemolysis from GNP-Dex treated red blood cells was estimated by a method developed by McNeil *et al.*²⁸. One ml of whole blood (Biochemed, Winchester, VA) was centrifuged at 2500 rpm for 10 minutes, and the blood cell (RBC and WBC) components were separated from the plasma constituents. The blood cell component was carefully resuspended in 1.5 ml of phosphate buffer saline containing 1 mg/ml, 7 mg/ml and 10 mg/ml GNP-Dex respectively. The separated blood cells were treated with GNP-Dex for 45 minutes following which the cells and GNP-Dex mixture were centrifuged at 2500 rpm for 10 minutes. The supernatants solutions were removed, ferricyanide in presence of bicarbonate was added to it, and incubated for 5 minutes. The absorbance of this mixture was measured at 540 nm using an Evolution 300 UV-VIS Spectrophotometer (Thermo Scientific, West Palm Beach, FL). Cells treated with phosphate buffered saline were utilized as the negative control and cells treated with a known hemolytic agent Triton X 100 (1%) for 45 minutes were used as positive control.

Vasoactivity. Animal model. All animal experiments were performed according to policies and procedures of Stony Brook University Institutional Animal Care and Use Committee after their approval of the protocol. Male hamsters (100 ± 4 days, mean ± SD, 112.5 ± 10 grams, n = 8) were anesthetized with isoflurane (4% induction, 1% thereafter). The left cheek pouch tissue was exteriorized, pinned across a Lucite pedestal and cleared of connective tissue^{48,51,52,55}. Physiological saline flowed over the exteriorized tissue (5 ml/min). The arcade – terminal arteriolar network junction was the microvascular observation site, as described previously²⁶. The site was visualized with a modified Nikon microscope (25 × objective), videorecorded using a Dage-MTI Gen/Sys CCD camera and a SVHS Panasonic AG7350 recorder. Diameter measurements of arterioles were made offline, calibrated with a stage micrometer. The final optical resolution was 0.7 µm, and magnification for diameter measures was 600 ×. At this level of the microcirculation, the vascular smooth muscle cells form a discontinuous layer on the abluminal side of the arteriole, revealing the outer surface of the inner endothelial cell layer. Thus exposure to the abluminal surface applies agents to both vascular smooth muscle cells and endothelial cells. By using localized abluminal exposure (instead of systemic intravenous exposure), several doses can be independently tested within the same animal as a screening assay for effect on the microcirculation as a whole. These vessels were deliberately chosen because they are the terminal resistance arterioles that directly control nutrient delivery to the capillaries.

Experimental protocol. Following a 30 minute resting period, baseline vasoactive responses to adenosine, acetylcholine and phenylephrine (10^{-4} mol/L each, micropipette application for 60 s, 5 min washout) confirmed that the arterioles had vasoactive tone. Micropipette contents were ejected from the micropipette tip (10–20 µm tip diameter) pneumatically, using the lowest pressure that ejected the contents; all pipettes contained a fluorescent tracer of FITC-BSA (fluorescein conjugated to bovine serum albumin, 4 kD, 10^{-6} mol/L) to confirm exposure location⁵⁷. GNP-Dex formulations were applied in increasing dosages (0, 0.1, 0.5, 2.6, 10, 50 mg/ml) via micropipette, using 30 s exposures, with a 5 min washout between dosages. The dosage of 0 mg/ml was vehicle only (saline with FITC-BSA). In three animals we tested the GNP biocompatibility coating, dextran (10 kD) alone using 3.5 or 35 mg/ml dextran in saline with FITC-BSA. Fifteen minutes later adenosine, acetylcholine and phenylephrine were again applied. The range of doses of GNP formulations was



chosen based on prior work in which the dilution effect of a bolus dose was directly measured³⁰; this is further expanded in the Discussion.

Statistics. All *in vitro* data are presented as mean \pm standard deviation. ($n = 4$) and $n = 6$ for histamine release assay. Student's t-test was used to analyze the differences among groups. Analysis of variance (ANOVA) for repeated measures was used for multiple comparisons between groups (dose response). For the *in vivo* studies, $n = 8$ was used and two or three independent observation sites were tested per animal. Diameters (μm) are reported for the baseline values. Diameter change is percent baseline: $[\text{peak change} - \text{baseline}]/[\text{baseline}] \times 100$. Data of figure 7B was analyzed using the sigmoidal dose response fit weighted by the standard deviation in OriginPro (v7.0383, Origin Labs, Inc. Northampton, MA); the EC_{50} and maximal response are given. Data of figure 7C was analyzed by ANOVA, using standard equations as found in Snedecor & Cochran⁵⁸. All statistical analyses were performed using a 95% confidence interval ($p < 0.05$).

- Zhang, Y., Nayak, T. R., Hong, H. & Cai, W. Graphene: A versatile nanoplatform for biomedical applications. *Nanoscale*. **4**, 3833–42 (2012).
- Shao, Y. *et al.* Graphene Based Electrochemical Sensors and Biosensors: A Review. *Electroanalysis*. **22**, 1027–36 (2010).
- Mullick Chowdhury, S. *et al.* Cell specific cytotoxicity and uptake of graphene nanoribbons. *Biomaterials*. **34**, 283–93 (2013).
- Sun, X. *et al.* Nano-graphene oxide for cellular imaging and drug delivery. *Nano Res.* **1**, 203–12 (2008).
- Paratala, B. S., Jacobson, B. D., Kanakia, S., Francis, L. D. & Sitharaman, B. Physicochemical characterization, and relaxometry studies of micro-graphite oxide, graphene nanoplatelets, and nanoribbons. *PLOS ONE*. **7**, e38185 (2012).
- Depan, D., Shah, J. & Misra, R. D. K. Controlled release of drug from folate-decorated and graphene mediated drug delivery system: Synthesis, loading efficiency, and drug release response. *Mater. Sci. Eng C*. **31**, 1305–12 (2011).
- Yang, X. *et al.* Multi-functionalized graphene oxide based anticancer drug-carrier with dual-targeting function and pH-sensitivity. *J. Mater. Chem.* **21**, 3448–54 (2011).
- Zhang, L. *et al.* Enhanced chemotherapy efficacy by sequential delivery of siRNA and anticancer drugs using PEI-grafted graphene oxide. *Small*. **7**, 460–4 (2011).
- Feng, L., Zhang, S. & Liu, Z. Graphene based gene transfection. *Nanoscale*. **3**, 1252–7 (2011).
- Lalwani, G. *et al.* Fabrication and characterization of three-dimensional macroscopic all-carbon scaffolds. *Carbon*. **53**, 90–100 (2013).
- Lalwani, G. *et al.* Two-Dimensional nanostructure-reinforced biodegradable polymeric nanocomposites for bone tissue engineering. *Biomacromolecules*. **14**, 900–9 (2013).
- Robinson, J. T. *et al.* Ultrasmall reduced graphene oxide with high near-infrared absorbance for photothermal therapy. *J. Am. Chem. Soc.* **133**, 6825–31 (2011).
- Huang, P. *et al.* Folic acid-conjugated graphene oxide loaded with photosensitizers for targeting photodynamic therapy. *Theranostics* 240–50 (2011).
- Yang, K. *et al.* Graphene in mice: Ultrahigh *in vivo* tumor uptake and efficient photothermal therapy. *Nano Letters*. **10**, 3318–23 (2010).
- Singh, S. K. *et al.* Thrombus inducing property of atomically thin graphene oxide sheets. *ACS Nano*. **5**, 4987–96 (2011).
- Sasidharan, A. *et al.* Differential nano-bio interactions and toxicity effects of pristine versus functionalized graphene. *Nanoscale*. **3**, 2461–4 (2011).
- Chang, Y. *et al.* *In vitro* toxicity evaluation of graphene oxide on A549 cells. *Toxicol. Lett.* **200**, 201–10 (2011).
- Yang, K. *et al.* *In vivo* pharmacokinetics, long-term biodistribution, and toxicology of PEGylated graphene in mice. *ACS Nano*. **5**, 516–22 (2010).
- Wang, K. *et al.* Biocompatibility of graphene oxide. *Nanoscale. Res. Lett.* **6**, 8 (2011).
- Liu, Z., Tabakman, S., Welsher, K. & Dai, H. Carbon nanotubes in biology and medicine: *In vitro* and *in vivo* detection, imaging and drug delivery. *Nano Res.* **2**, 85–120 (2009).
- Bianco, A., Kostarelos, K., Partidos, C. D. & Prato, M. Biomedical applications of functionalised carbon nanotubes. *Chem. Comm.* **0**, 571–7 (2005).
- Kanakia, S. *et al.* Physicochemical characterization of a novel graphene-based magnetic resonance imaging contrast agent. *Int. J. Nanomed.* **8**, 2821–2833 (2013).
- Nath, N., Lowery, C. & Niewiarowski, S. Antigenic and antiheparin properties of human platelet factor 4 (PF4). *Blood*. **45**, 537–50 (1975).
- Fosbrink, M., Niculescu, F. & Rus, H. The role of C5b-9 terminal complement complex in activation of the cell cycle and transcription. *Immunol. Res.* **31**, 37–46 (2005).
- Sundsmo, J. S. & Wood, L. M. Activated factor B (Bb) of the alternative pathway of complement activation cleaves and activates plasminogen. *J. Immunol.* **127**, 877–80 (1981).
- Tedgui, A. & Mallat, Z. Cytokines in Atherosclerosis: Pathogenic and Regulatory Pathways. *Physiological Reviews*. **86**, 515–81 (2006).
- Thakur, A. *et al.* Balance of Pro- and Anti-Inflammatory Cytokines Correlates with Outcome of Acute Experimental Pseudomonas aeruginosa Keratitis. *Infection and Immunity*. **70**, 2187–97 (2002).
- Dobrovolskaia, M. A. *et al.* Method for analysis of nanoparticle hemolytic properties *in vitro*. *Nano Letters*. **8**, 2180–7 (2008).
- Williams, D. F. On the mechanisms of biocompatibility. *Biomaterials*. **29**, 2941–53 (2008).
- Rivers, R. J., Beckman, J. B. & Frame, M. D. Technique for using video microscopy and indicator dilution for repeated measurements of cardiac output in small animals. *Anesthesiology*. **94**, 489–95 (2001).
- Moodley, L., Mongar, J. L. & Foreman, J. C. Histamine release induced by dextran: The nature of the dextran receptor. *Eur. J. Pharmacol.* **83**, 69–81 (1982).
- Dvorak, A. M. & Galli, S. J. Antigen-induced, IgE-mediated degranulation of cloned immature mast cells derived from normal mice. *Am. J. Pathol.* **126**, 535–45 (1987).
- Wu, K. K. & Hoak, J. C. Increased platelet aggregates in patients with transient ischemic attacks. *Stroke*. **6**, 521–4 (1975).
- Radomski, A. *et al.* Nanoparticle-induced platelet aggregation and vascular thrombosis. *Br. J. Pharmacol.* **146**, 882–93 (2005).
- Chanan-Khan, A. *et al.* Complement activation following first exposure to pegylated liposomal doxorubicin (Doxil®): possible role in hypersensitivity reactions. *Ann. Oncol.* **14**, 1430–7 (2003).
- Tan, X. *et al.* Functionalization of Graphene Oxide Generates a Unique Interface for Selective Serum Protein Interactions. *ACS Applied Materials & Interfaces*. **5**, 1370–7 (2013).
- Reynolds, R. *et al.* Plasma complement components and activation fragments: Associations with age-related macular degeneration genotypes and phenotypes. *Invest. Ophthalmol. Vis. Sci.* **50**, 5818–27 (2009).
- Bertholon, I., Vauthier, C. & Labarre, D. Complement activation by core-shell poly(isobutylcyanoacrylate)-polysaccharide nanoparticles: Influences of surface morphology, length, and type of polysaccharide. *Pharm. Res.* **23**, 1313–23 (2006).
- Barton, G. M. A calculated response: control of inflammation by the innate immune system. *The Journal of Clinical Investigation*. **118**, 413–20 (2008).
- Lacy, P. & Stow, J. L. Cytokine release from innate immune cells: association with diverse membrane trafficking pathways. *Blood*. **118**, 9–18 (2011).
- Yue, H. *et al.* The role of the lateral dimension of graphene oxide in the regulation of cellular responses. *Biomaterials*. **33**, 4013–21 (2012).
- Nemunaitis, J. F. T., Shabe, P., Martineau, D. & Ando, D. Comparison of serum interleukin-10 (IL-10) levels between normal volunteers and patients with advanced melanoma. *Cancer Invest.* **19**, 239–47 (2001).
- Alecu, M. G. L., Coman, G. & Galatescu, L. The interleukin-1, interleukin-2, interleukin-6 and tumour necrosis factor alpha serological levels in localised and systemic sclerosis. *Rom J Intern Med.* **36**, 251–9 (1998).
- Barshtein, G., Arbell, D. & Yedgar, S. Hemolytic effect of polymeric nanoparticles: Role of albumin. *IEEE. Trans. Nanobioscience*. **10**, 259–61 (2011).
- Meng, J. *et al.* Effects of long and short carboxylated or aminated multiwalled carbon nanotubes on blood coagulation. *PLOS ONE*. **7**, e38995 (2012).
- Liao, K.-H., Lin, Y.-S., Macosko, C. W. & Haynes, C. L. Cytotoxicity of graphene oxide and graphene in human erythrocytes and skin fibroblasts. *ACS Appl. Mater. Interfaces*. **3**, 2607–15 (2011).
- Frame, M. D. *et al.* Diminished arteriolar responses in nitrate tolerance involve ROS and angiotensin II. *Am. J. Physiol. Heart. Circ. Physiol.* **282**, H2377–H85 (2002).
- Frame, M. D. & Mabanta, L. Remote microvascular preconditioning alters specific vasoactive responses. *Microcirculation*. **14**, 739–51 (2007).
- Frame, M. D. & Sarelius, I. H. L-arginine-induced conducted signals alter upstream arteriolar responsiveness to L-arginine. *Circ. Res.* **77**, 695–701 (1995).
- Frame, M. D. & Sarelius, I. H. Endothelial cell dilatory pathways link flow and wall shear stress in an intact arteriolar network. *J. Appl. Physiol.* **81**, 2105–14 (1996).
- Mabanta, L., Valane, P., Borne, J. & Frame, M. D. Initiation of remote microvascular preconditioning requires K(ATP) channel activity. *Am. J. Physiol. Heart. Circ. Physiol.* **290**, H264–H71 (2006).
- Mustafa, S. S., Rivers, R. J. & Frame, M. D. Microcirculatory basis for nonuniform flow delivery with intravenous nitroprusside. *Anesthesiology*. **91**, 723–31 (1999).
- Frame, M. D., Dewar, A. M., Mullick Chowdhury, S. & Sitharaman, B. Vasoactive effects of aqueous suspensions of single walled carbon nanotubes in hamsters and mice. *Nanotoxicology*. in press (2013).
- Nakatani, K. *et al.* Inhibitions of histamine release and prostaglandin E₂ synthesis by mangosteen, a thai medicinal plant. *Biol. Pharm. Bull.* **25**, 1137–41 (2002).
- Frame, M. D., Rivers, R. J., Altland, O. & Cameron, S. Mechanisms initiating integrin-stimulated flow recruitment in arteriolar networks. *J. Appl. Physiol.* **102**, 2279–87 (2007).
- Dewar, A. M., Clark, R. A., Singer, A. J. & Frame, M. D. Curcumin mediates both dilation and constriction of peripheral arterioles via adrenergic receptors. *J. Invest. Dermatol.* **131**, 1754–60 (2011).
- Georgi, M. K., Dewar, A. M. & Frame, M. D. Downstream exposure to growth factors causes elevated velocity and dilation in arteriolar networks. *J. Vasc. Res.* **48**, 11–22 (2011).
- Snedecor, G. W. & Cochran, W. G. *Statistical Methods*. The Iowa State University Press; 1974.

Acknowledgements

This work was supported by Wallace H Coulter Foundation, Stony Brook School of Medicine and the Office of the Vice President for Research. The authors thank Ms. Shelagh Zegers for her help with lyophilization.



Author contributions

S.M.C., S.K., J.T., M.D.F., A.M.D. and B.S. designed the experiments. S.M.C., A.M.D., M.D.F. carried out the experiments and calculations. S.M.C., S.K., J.T., M.D.F., K.P.S., W.M. and B.S. wrote and edited the paper.

Additional information

Competing financial interests: The authors declare no competing financial interests.

How to cite this article: Chowdhury, S.M. *et al.* *In Vitro* Hematological and *In Vivo* Vasoactivity Assessment of Dextran Functionalized Graphene. *Sci. Rep.* 3, 2584; DOI:10.1038/srep02584 (2013).



This work is licensed under a Creative Commons Attribution-NonCommercial-ShareAlike 3.0 Unported license. To view a copy of this license, visit <http://creativecommons.org/licenses/by-nc-sa/3.0>